07 - 10 September 2009

PROCEEDINGS

54. IWK

Internationales Wissenschaftliches Kolloquium
International Scientific Colloquium

Information Technology and Electrical Engineering - Devices and Systems, Materials and Technologies for the Future

Faculty of Electrical Engineering and Information Technology

Startseite / Index:
http://www.db-thueringen.de/servlets/DocumentServlet?id=14089

TECHNISCHE UNIVERSITÄT
ILMENAU

Impressum

Herausgeber: Der Rektor der Technischen Universität Ilmenau
Univ.-Prof. Dr. rer. nat. habil. Dr. h. c. Prof. h. c.
Peter Scharff

Redaktion: Referat Marketing
Andrea Schneider

Fakultät für Elektrotechnik und Informationstechnik
Univ.-Prof. Dr.-Ing. Frank Berger

Redaktionsschluss: 17. August 2009

Technische Realisierung (USB-Flash-Ausgabe):
Institut für Medientechnik an der TU Ilmenau
Dipl.-Ing. Christian Weigel
Dipl.-Ing. Helge Drumm

Technische Realisierung (Online-Ausgabe):
Universitätsbibliothek Ilmenau
ilmedia
Postfach 10 05 65
98684 Ilmenau

Verlag:
Verlag ISLE, Betriebsstätte des ISLE e.V.
Werner-von-Siemens-Str. 16
98693 Ilmenau

© Technische Universität Ilmenau (Thür.) 2009

Diese Publikationen und alle in ihr enthaltenen Beiträge und Abbildungen sind urheberrechtlich geschützt.

ISBN (USB-Flash-Ausgabe): 978-3-938843-45-1
ISBN (Druckausgabe der Kurzfassungen): 978-3-938843-44-4

Startseite / Index:
http://www.db-thueringen.de/servlets/DocumentServlet?id=14089

A NEW NETWORK CALCULATION MODEL FOR THE PREDETERMINATION OF THE EXCITATION CURRENT AND THE REACTANCE OF SALIENT – POLE SYNCHRONOUS MACHINES

Marcus Banda, Dr. Olaf Michelsson

Siemens AG, Energy Sector
Generator Plant Erfurt, Germany

ABSTRACT

The goal of this project is to calculate the characteristic field currents and reactance of salient-pole synchronous machines. In the paper presented a new extended calculation model basing on a magnetic circuit is developed. Field saturation and the field in the pole gap are naturally taken into account. Additionally a method for the quick predetermination of the rated load excitation current within an iterative loop is presented. The Magnetic Circuit is then applied to two four-pole machines with an apparent power of 42.5MVA and 55MVA having rated voltages of 10.5kV.

Index Terms **–** salient-pole synchronous machine, determination of excitation current, reactance, network model, magnetic circuit simulation using spice

1. INTRODUCTION

Synchronous machines have a wide variety of applications. An important objective of synchronous generators is to provide electrical energy for the people and for the industry. These synchronous generators mainly differ in their rotor construction. This work focuses on large and fast rotating salient pole machines with a concentrated field winding. The correct calculation of its magnetic circuit causes difficulties. This calculation is important because it is the precondition for the following thermal and mechanical design. The aim of this work is to optimize the magnetic circuit calculation and determining the field current and the reactance more precisely. The model presented bases on an electric – magnetic analogy network consisting of sources and nonlinear resistive elements. In the first approach a two-dimensional model of the machine is created, assuming no axial flux distribution. End- effects like the end-winding inductance is added separately afterwards. The model environment is realized in FORTRAN code to handle all input geometry, boundary condition and excitation. The created netlist is then solved with spice and the results are read into the program again where the magnetic flux is evaluated. In contrast to a finite element analysis of the field, all magnetic quantities are obtained directly from the calculation without deriving them from e.g. the vector potential.

2. THE MAGNETIC CIRCUIT

For the balanced operation mode of a rotating salient-pole synchronous machine a static analysis of the machine flux and current provides a complete description, neglecting eddy current effects. Referring to the scalar Magnetic Flux Law formulation with the magnetic field strength H integrated along a closed path L results in the magneto motive force Θ:

$$\oint_L H \cdot dl = \Theta \qquad (2.1)$$

With (2.1) a basis for the electric-magnetic equivalent circuit is found. Discretising the closed-loop integral in (2.1) to a sum of magnetic voltages V_i leads to an equivalent circuit with lumped elements. In (2.2) these elements are separated into linear magnetic resistances R_m and nonlinear parts depending on the flux Φ.

$$\sum_k H_k \cdot \Delta l_k = \sum_k V_k = \sum_i R_{m,i} \cdot \Phi_i + \sum_j V_j(\Phi_j) \qquad (2.2)$$

where k sums up to k=i+j.

In the magnetic network examined, the stator and the rotor as the main elements of the machine are represented by several nonlinear magnetic resistances, as can be seen in *Figure 3*. In contrast to the solid shaft, the material curve for the stator core has to be sheared to consider the air ducts. Therefore a new magnetic flux density $B_{FE,new}$ is calculated in (2.3) from the original characteristic with a $B_{FE,orig}$ vs. H correlation:

$$B_{FE,new} = \mu_0 \cdot H_{FE} \cdot (1 - k_{FE}) + B_{FE,orig} \cdot k_{FE} \qquad (2.3)$$

with k_{FE} characterizing the stacking of the stator lamination and the coating. An example is displayed in *Figure 1*.

© 2009 - 54th Internationales Wissenschaftliches Kolloquium

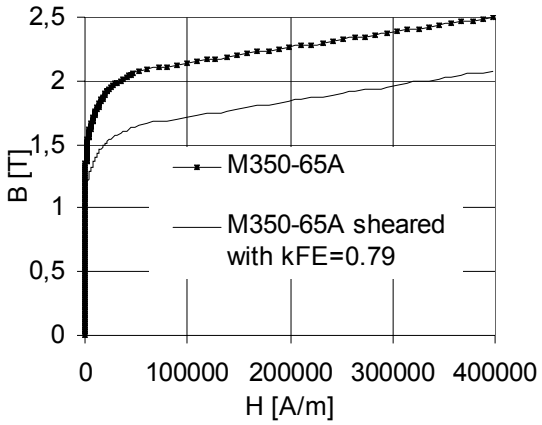

Figure 1: sheared magnetization curve of stator material

The current in the windings in the two main elements excite the magnetic circuit as magneto motive forces (mmfs) and are regarded as voltage sources. Consequently the concentrated field winding is represented by a couple of voltage sources in the middle of the pole shaft, whereas the distributed two-layer winding in the stator is modeled with sources in the stator teeth as shown in *Figure 2*. The basic model in *Figure 2* comprises one slot pitch and is duplicated times the number of slots as can be seen in *Figure 3*.

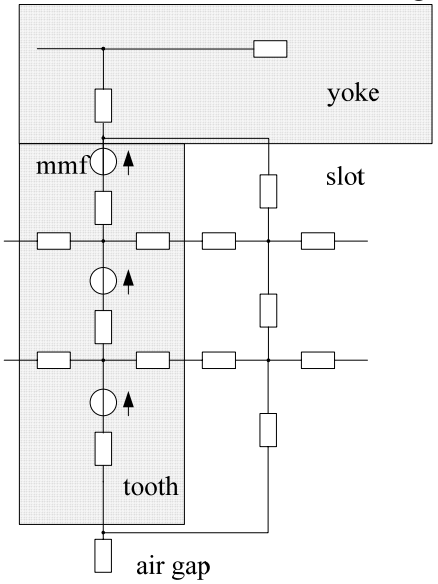

Figure 2: basic element for one stator slot pitch

To consider the current in the distributed stator winding, the fundamental wave of the magneto motive force is considered.
The separate network branches of the stator and rotor are then combined in the air-gap via a four layer interpolation network.

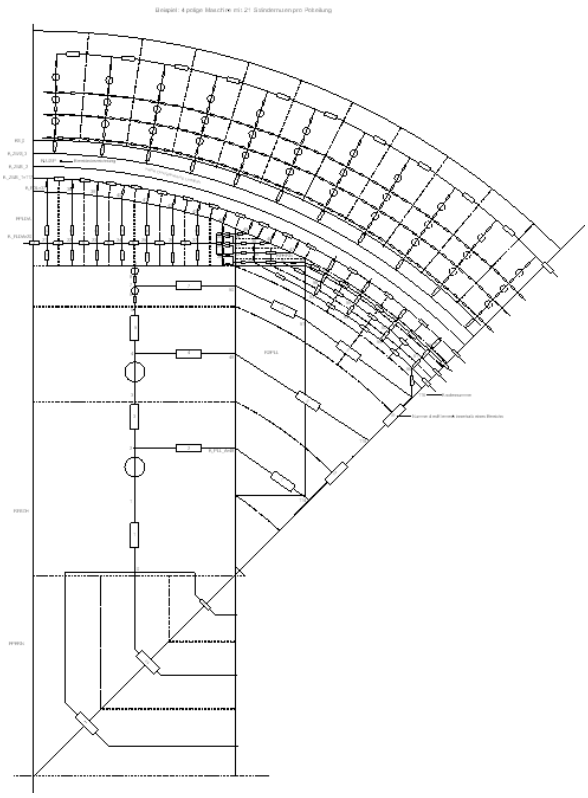

Figure 3: network for half a pole pitch

3. DETERMINATION OF EXCITATION CURRENTS

3.1. No-Load Characteristic

In the existing model the no-load characteristic is obtained by raising the field current I_F of the machine and evaluating the corresponding line-to-line voltage U_{LL} at the open stator terminals. However the determination of the stator voltage needs a few more intermediate steps within the static analysis. As the first step the rotor mmf in the loop integral of a flux line is summed up to

$$\Theta_F = 2 \cdot w_p \cdot I_F \qquad (3.1)$$

with w_p as the number of turns per pole

Now obtaining the flux Φ_i and the magnetic voltages V_i from the solved network, the radially directed magnetic flux density B_i for each element in the height of the stator winding is determined. Following the two-axis theory the calculated quantities are separated in a direct-axis and a quadrature-axis component. Each Fundamental Wave $\hat{B}_{(1)}$ of the Fourier analyzed component is then integrated over the cross sectional surface to the flux as follows:

$$\hat{\Phi}_{(1)d} = \int_{l=0}^{l_m} \int_{x=-\frac{\tau}{2}}^{x=+\frac{\tau}{2}} \hat{B}_{(1)d} \cdot \cos\left(\frac{x}{\tau} \cdot \pi\right) \cdot dx \cdot dl \qquad (3.2)$$

with $\tau = \frac{2 \cdot \pi \cdot r}{2 \cdot p}$ being the pole pitch at the current radius r in height of the stator winding and p as the number of pole pairs
With that (3.2) finally results in

$$\hat{\Phi}_{(1)d} = \frac{2 \cdot \tau}{\pi} \cdot l_m \cdot \hat{B}_{(1)d} \quad (3.3)$$

This procedure is similarily done for the quadrature axis. Combing the components of the flux, the induced line-to-line voltage is determined with the following equation:

$$U_{(1),LL} = \sqrt{3} \cdot 2\pi f_N \cdot w_S \xi_{(1)} \cdot \frac{1}{\sqrt{2}} \sqrt{\hat{\Phi}_{(1),d}^2 + \hat{\Phi}_{(1),q}^2} \quad (3.4)$$

with f_N as the nominal frequency, w_s the number of turns per stator phase and $\xi_{(1)}$ as the winding factor of the fundamental wave

In *Figure 4, Figure 5* and *Table 1*, *Table 2* three different possibilities of calculating the no-load characteristic are displayed. The Magnetic Circuit method is in good agreement with the finite element solution with FEMAG on the one hand and the measured curve from the shop test on the other hand.

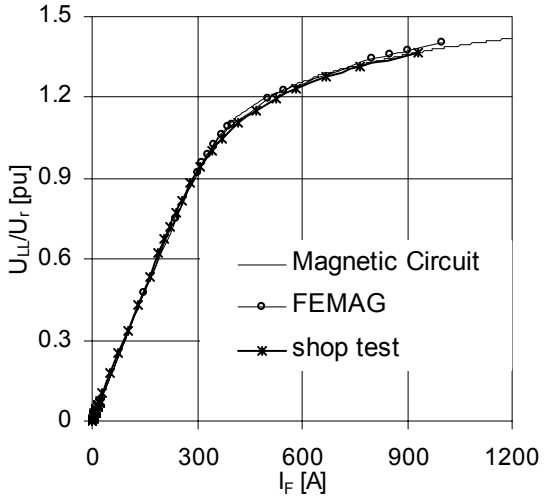

Figure 4: No-load Characteristic of a SGen-100A-4p (No 1) generator

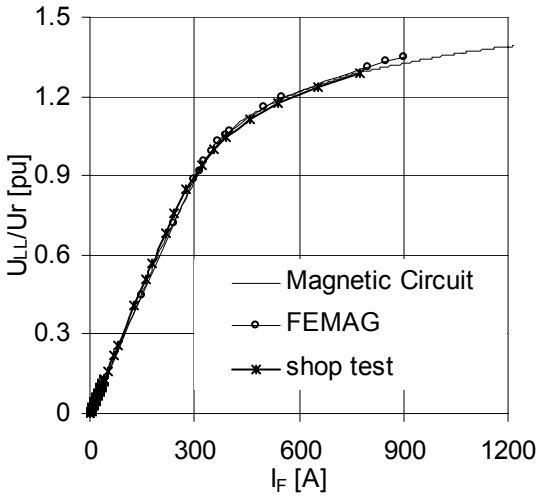

Figure 5: No-load Characteristic of a SGen-100A-4p (No 3) generator

3.2. Short-Circuit Characteristic

The short circuit characteristic is simply a straight line passing through the short circuit operating point and the origin of the coordinate system with the quantities stator current I_S and field current I_F. This behavior is caused by the displacement of the flux onto the stray paths thus effecting a negligible saturation only. As mentioned in section 1 stator end effects have to be considered as soon as a stator current flows. Therefore the end-winding stray inductance $X_{\sigma W}$ is given by [2]. The same procedure as specified in section 3.1 is applied except for the consideration of the stator current. The objective changes in finding the excitation current that causes zero stator terminal voltage. The results are examined in *Table 1* and *Table 2,* which show a good agreement to the measurement, again.

Table 1: comparison of calculated and measured no-load (nl) and short – circuit (sc) excitation current of SGen-100A-4p (No 3)

	shop test	MC	FEMAG
$I_{F,nl}$/A	358.0	356.6	355.0
$I_{F,sc}$/A	694.4	702.4	-

Table 2: comparison of calculated and measured no-load and short – circuit excitation current of SGen-100A-4p (No 1)

	shop test	MC	FEMAG
$I_{F,nl}$/A	340,6	333.8	340.0
$I_{F,sc}$/A	623.4	629,1	-

3.3. Rated Load Excitation

The rated load case is defined by the stator line-to-line voltage, stator current and the given power factor cosφ. Within the Magnetic Circuit the two degrees of freedom identified as the exciter current I_F and the angle ε [1]. ε defines the position of the stator space

phasor $\underline{I}_S$ against the d-axis as displayed in *Figure 6*. The value of the stator current I_S is determined by its rated value I_r with the rated apparent power S_r and the rated line-to-line voltage U_r as follows:

$$I_S = I_r = \frac{S_r}{\sqrt{3} \cdot U_r} \tag{3.5}$$

According to the no-load case the field current is raised stepwise while ε is kept constant in one cycle. The initial value of ε is calculated from the relations pointed out in *Figure 6*. After that the sum of the three angles must be 90°:

$$\vartheta + \varepsilon + \varphi = 90° \tag{3.6}$$

In contrast to φ which is determined by the power factor, the pole angle ϑ can be taken from the following approach. The stator voltage and stator current can be split into their direct- axis and quadrature-axis components as follows:

$\underline{U}_S = U_d + jU_q$ and $\underline{I}_S = I_d + jI_q$.

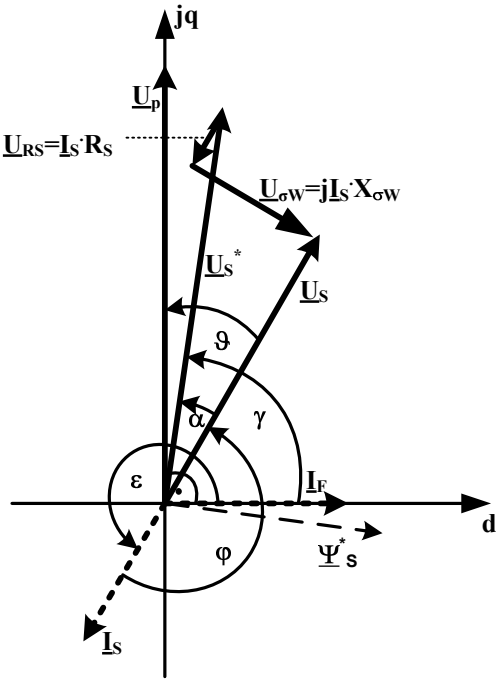

Figure 6: Vector diagram of the machine during load operation in the d-q plane

Furthermore the quadrature – axis reactance X_q results from the flux linkage of the q –axis Ψ_q, the angular speed ω and the corresponding quadrature-axis current I_q:

$$X_q = \frac{\omega \cdot \Psi_q}{I_q} \tag{3.7}$$

Equation (3.7) could be rewritten with

$$\omega \cdot \Psi_q = -U_s \cdot \cos(\frac{\pi}{2} - \vartheta) \tag{3.8}$$

and

$$I_q = I_S \cdot \sin\varepsilon \tag{3.9}$$

and bearing (3.6) in mind (3.7) finally results in :

$$X_q = -\frac{U_S \cdot \sin\vartheta}{I_s \cdot (\cos\varphi \cdot \cos\vartheta - \sin\varphi \cdot \sin\vartheta)} \tag{3.10}$$

After some transpositions (3.10) becomes:

$$\vartheta = \arctan\left(\frac{\cos\varphi}{\sin\varphi - \frac{U_s}{I_s \cdot X_q}}\right) \tag{3.11}$$

With given quantities φ, $U_s = \frac{U_r}{\sqrt{3}}$ and I_s only a value for the quadrature – axis reactance has to be found. For X_q the unsaturated value as shown in section 4.1 is taken for the load case iteration. Now ε can be evaluated from (3.6) and (3.11) for each cycle.
Having solved the network equations, the solution quantities for the two dimensional model, marked with a *, have to be corrected with the end-winding stray inductance and the resistance for the stator AC losses in the following way. As can be seen in *Figure 6* the stator voltage phasor $\underline{U}^*_S$ with its components U_d^* and U_q^* result from the network solution, similar to (3.4). Therewith the magnitude U_S^* and the angle γ will be derived as follows:

$$U_S^* = \sqrt{U^*d^2 + U^*q^2} \tag{3.12}$$

and

$$\gamma = \arctan\left(\frac{U^*q}{U^*d}\right) \tag{3.13}$$

Consequently the stator space phasor voltage is expressed to:

$$\underline{U}_S = U^*_S \cdot e^{j\gamma} + I_S \cdot e^{j\varepsilon} \cdot \left(R_S + jX_{\sigma W}\right) \tag{3.14}$$

Power factor angle φ can be checked using (3.15):

$$\varphi = \gamma - \varepsilon - \alpha \tag{3.15}$$

Angle α is obtained from the vector diagram in *Figure 6*. (strongly exaggerated)

$$\alpha = \gamma - \arctan\left(\frac{U^*_S \cdot \sin\gamma + I_S \cdot \left(R_S \cdot \sin\varepsilon + X_{\sigma W} \cdot \sin(\varepsilon + \frac{\pi}{2})\right)}{U^*_S \cdot \cos\gamma + I_S \cdot \left(R_S \cdot \cos\varepsilon + X_{\sigma W} \cdot \cos(\varepsilon + \frac{\pi}{2})\right)}\right) \tag{3.16}$$

The pair of values with U_S and cosφ with the corresponding I_F and ε can now be compared to the rated values. If the deviation is greater than 1%, a new cycle is started with better initial values from the last step. In general this process converges quickly to

the final pair of values. *Figure 7* shows a comparison of obtained results for three different machines. Although a measurement during the shop test was not possible the finite element solution is taken as the reference.

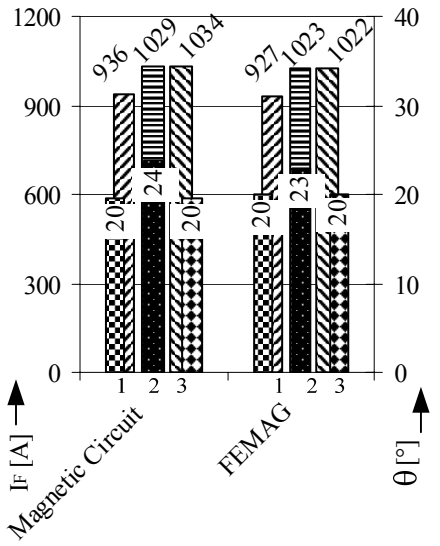

Figure 7: Comparison of calculated rated load excitation current and pole angle

Obviously the Magnetic Circuit method shows a very good agreement compared to the finite element solution in FEMAG.

4. DETERMINATION OF SYNCHRONOUS MACHINE REACTANCE

4.1. The synchronous reactance

The characteristic reactance for each of the two axis can be computed with the Magnetic Circuit method. The conditions for the calculation of the synchronous reactances with the model are given by (4.1) and (4.2), bearing in mind that the end-winding stray inductance has to be added afterwards:

$$X_d = \frac{\omega \cdot \Psi^*_d}{I_d} + X_{\sigma W} \mid I_q = I_F = 0 \qquad (4.1)$$

$$X_q = \frac{\omega \cdot \Psi^*_q}{I_q} + X_{\sigma W} \mid I_d = I_F = 0 \qquad (4.2)$$

Due to the nonlinear magnetization properties of the material, the inductances strongly depend on the current load or test condition. Therefore three different states are pointed out. Firstly, the unsaturated value with the iron being ideally permeable. Secondly, saturation occurs due to the no-load case. And finally, load saturation is mentioned, which differs from the no-load saturation because of the unsymmetrical saturation of the poles.

The formulas for the three different saturation states remain the same. Only the absolute values of the results differ. Therewith, the unsaturated and the no-load saturated values of the d-axis reactance (X_{du} and X_{ds}) are determined following the instructions in [3] with appropriate field currents. In contrast to that, we need to take a closer look at the load situation. In the direct-axis two flux components appear caused by the rotor and the stator flux linkage in (4.3). Consequently, the d-axis inductance L_d may not be computed directly.

$$\Psi_d = L_d \cdot I_d + L_{md} \cdot I'_F \qquad (4.3)$$

with L_{md} as the mutual inductance between the stator and the rotor circuit

For this reason all permeabilities of the magnetic resistances will be frozen to their values during the load case. After that the field current is set to zero and only the d-axis is excited by a current in the stator. As it can be seen in *Table 3,* the load saturated value is about 10% less the no-load saturated value obtained during the shop test, which is caused by the unsymmetrical pole saturation.

The unsaturated value of X_{qu} results from a mere stator current feeding similar to the d-axis reactance determination. In contrast to that the load saturated value X_{qs} can be calculated with the iterated magnetic wheel angle using (3.10).

4.2. The stator stray inductance

The stator stray reactance $X_{\sigma S}$ is computed with a certain assumption about the magnetic path of the flux. It is assumed that the pole and the lower half of the air – gap is blocked for magnetic flux of the stator stray field as can be seen in *Figure 8*. With the blocking, the magnetic resistance rises to infinite and the mutual part of the d- and q- axis reactances, X_{md} and X_{mq}, become zero. Again, the same equation for the reactance computation as in section 4.1 is used.

The reactance is assumed to stay unsaturated because of the high portion of air in the flux path.

$$X_{\sigma S} = \frac{\omega \cdot \Psi^*_d}{I_d} + X_{\sigma W} \mid X_{md} = X_{mq} = 0 \qquad (4.4)$$

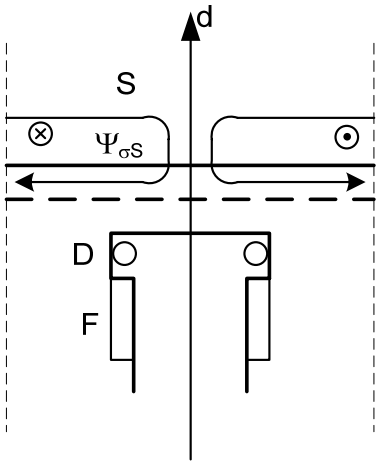

Figure 8: Flux line plot for the stator stray inductance, S: stator, D: damper, F: field

Table 3: comparison of evaluated reactance of SGen-100A-4p (No 3)

x/pu	MC	shop test
x_{du}	2,15	2,2
x_{qu}	1,05	-
x_{ds}	1,97	1,94
x_{ds}^{*}	1,77	-
x_{qs}	0,6	-
$x_{\sigma S}$	0,15	-

* this value is load saturated

5. CONCLUSION

With the Magnetic Circuit method (MC) the field current and the reactance are computed quickly and accurately compared to the more time-consuming finite-element analysis and it shows a very good agreement with the shop test results. Furthermore, geometric and load variations are done in minutes. In addition to that all internal fluxes can be extracted and processed to use it in an electric equivalent circuit.

6. APPENDIX

w_S number of turns per stator phase

$$w_S = \frac{z_S \cdot N_S}{2 \cdot m \cdot a_S}$$

with z_S as the number of conductors per slot, N_S the number of stator slots, m number of phases and a_s as the number of parallel branches

ζ_Z the spread factor

$$\xi_Z \approx \frac{3}{\pi} = 0,955$$

$\zeta_{S\nu}$ the winding pitch factor

$$\xi_{S\nu} = \sin(\nu \cdot \frac{\pi}{2} \cdot \frac{W_x}{N_\tau})$$

with N_τ as the number of slots per pole pitch and W_x as the winding pitch

for the fundamental wave $\nu = 1$, yields the winding factor

$$\xi_{(1)} = \xi_{(1),S} \cdot \xi_Z$$

7. REFERENCES

[1] Banda, M., Neues Netzwerk-Berechnungsmodell zur Vorausbestimmung des Erregerstromes und der Reaktanzen von Schenkelpol-Synchronmaschinen, diploma thesis, TU Dresden, Dresden, 2007.

[2] Vogt K., Berechnung rotierender elektrischer Maschinen, VEB Verlag Technik Berlin, 1988

[3] IEC 60034-4, 1998